

Outage Performance of Uplink Two-tier Networks Under Backhaul Constraints

Shirin Jalali, Zolfa Zeinalpour-Yazdi and H. Vincent Poor

Abstract—Multi-tier cellular communication networks constitute a promising approach to expand the coverage of cellular networks and enable them to offer higher data rates. In this paper, an uplink two-tier communication network is studied, in which macro users, femto users and femto access points are geometrically located inside the coverage area of a macro base station according to Poisson point processes. Each femtocell is assumed to have a fixed backhaul constraint that puts a limit on the maximum number of femto and macro users it can service. Under this backhaul constraint, the network adopts a special open access policy, in which each macro user is either assigned to its closest femto access point or to the macro base station, depending on the ratio between its distances from those two. Under this model, upper and lower bounds on the outage probabilities experienced by users serviced by femto access points are derived as functions of the distance between the macro base station and the femto access point serving them. Similarly, upper and lower bounds on the outage probabilities of the users serviced by the macro base station are obtained. The bounds in both cases are confirmed via simulation results.

Index Terms—Heterogeneous networks, Backhaul constraint, Uplink communication, Outage, Open access policy

I. INTRODUCTION

Fourth generation (4G) mobile communication standards such as LTE-advanced promise very high data rates. Enabling multi-tier networks is one of the methods that enables such standards to address the ever-increasing demand for higher data rates in cellular communication networks. In a multi-tier network, unlike the traditional design, multiple layers of cells, each serviced by a different type of base station, are employed simultaneously. In two-tier femtocell networks, for example, in addition to the traditional base stations, there are femto access points (FAPs) installed by users in their homes or offices. These additional base stations are connected to the cellular network through the users' broadband Internet connections. These FAPs expand the coverage of the main network to indoors and also reduce its load. However, the limited capacities of users broadband connections impose a backhaul constraint that limits the number of simultaneous users each femto cell can cover.

In this paper we study the outage performance of a two-tier uplink femtocell network. Macro users (MUs), femto users (FUs) and FAPs are assumed to be spatially distributed according to Poisson point processes (PPPs) [1]. Each femtocell

is assumed to have a limited backhaul capacity. Up to its capacity, each FAP employs a special *open access policy*, studied in [2] and [3] for downlinks. Based on this policy, each MU is serviced by its closest FAP if i) the ratio between its distance to its closet FAP and its distance to the MBS exceeds some threshold, and ii) the number of users already being serviced by that FAP is less than its capacity.

A. Related work

PPPs were originally suggested in [4]–[6] as a more tractable and realistic model for the locations of cells and users in a wireless network. The outage performance of two-tier networks under PPP distribution of users or access points is studied in [7]–[10] and in [10]–[16] for downlink and uplink communications, respectively. In none of these papers are the FAPs' backhaul constraints taken into account. In fact, to our knowledge, while there have been studies of the effects of femtocell backhaul constraints on other aspects of networks, there has been no prior analytical work on their effects on the users' outage performance in a two-tier network. (Refer to [17]–[20] as a sample of some recent results.) In this paper, we extend the analysis of uplink two-tier networks presented in [15] to the case in which each FAP has a backhaul constraint that limits the number of users it can service. We derive analytical upper and lower bounds on the outage probabilities experienced by the users serviced by the FAPs.

B. Notation

Sets are denoted by calligraphic letters such as \mathcal{A} and \mathcal{B} . The size of a set \mathcal{A} is denoted by $|\mathcal{A}|$. The Laplace transform of random variable X is denoted by $\Phi_X(s) \triangleq \mathbb{E}[e^{-sX}]$. Given $x \in \mathbb{R}$, $(x)^+ \triangleq \max(x, 0)$. Throughout the paper, $\mathcal{P}(s, x)$ denotes the cumulative distribution function of a gamma random variable with shape parameter s and scale parameter 1. Given a Poisson random variable X with parameter λ , $\mathbb{P}(X \leq k) = e^{-\lambda} \sum_{i=0}^k \frac{\lambda^i}{i!} = 1 - \mathcal{P}(k+1, \lambda)$.

C. Paper organization

The paper is organized as follows. Section II reviews the system model including the employed modulation, users and FAPs spatial distributions, and the access policy. The distributions of number of users falling into different service groups are studied in Section III. Section IV studies the outage probability experienced by the MUs serviced by FAPs. Similarly, Section V analyzes the outage probability experienced by the MUs serviced by the MBS. Section VI presents numerical results and, finally, Section VII concludes the paper.

S. Jalali is with the Department of Electrical Engineering, Princeton University, NJ 08540 (e-mail: sjalali@princeton.edu),

Z. Zeinalpour-Yazdi is with the Department of Electrical and computer Engineering, Yazd University, Yazd, Iran (e-mail: zeinalpour@yazd.ac.ir),

H. V. Poor is with the Department of Electrical Engineering, Princeton University, NJ 08540 (e-mail: poor@princeton.edu).

II. SYSTEM MODEL

A. MCFH technique

Both macro and femto users are assumed to employ multicarrier frequency-hopping (MCFH) modulation introduced in [21]. In MCFH the available bandwidth is divided into n_s non-overlapping subbands and each subband is divided into n_h equispaced frequencies, respectively. Hence, there are overall $n_s n_h$ available orthogonal subchannels. During each time slot, each user selects n_s subchannels by independently and uniformly at random choosing one subchannel from each subband. While MCFH modulation is very similar to orthogonal frequency division modulation (OFDM), unlike OFDM it does not require centralized frequency assignment. Hence, while, with some minor adjustments, the results derived under this modulation are also applicable to networks employing OFDM, MCFH modulation is much better suited for analytical performance studies.

B. Spatial distribution

Consider MBS b_m located at the center of a circle of radius R denoted by \mathcal{S}_m . \mathcal{A}_f , \mathcal{U}_m and \mathcal{U}_f denote the set of FAPs, MUs and FUs, respectively. Conditioned on the locations of the FAPs \mathcal{A}_f , FUs and MUs are distributed according to independent PPPs. FAPs and MUs are drawn according to PPPs of densities λ_f and μ_m , respectively. Let \mathcal{U}_m , $N_m = |\mathcal{U}_m|$, and $\bar{n}_{mu} = E[N_m] = \pi R^2 \mu_m$ denote the set of MUs in \mathcal{S}_m , the number of MUs and the expected number of MUs, respectively. Similarly, let \mathcal{A}_f , $N_{a_f} = |\mathcal{A}_f|$, and $\bar{n}_{fap} = E[N_{a_f}] = \pi R^2 \lambda_f$ denote the set of FAPs in \mathcal{S}_m , the number of FAPs and the expected number of FAPs, respectively. The FUs corresponding to each FAP $a_f \in \mathcal{A}_f$ are distributed according to a PPP with density μ_f in a disk of width δ and inner radius of r_f centered at a_f . By this construction, the expected number of FUs served by a femto cell is equal to $\bar{n}_{fu} = \pi((r_f + \delta)^2 - r_f^2)\mu_f$.

Given FAP $a_f \in \mathcal{A}_f$, $\mathcal{U}_f(a_f)$ and $\mathcal{U}_m(a_f)$ denote the set of FUs and MUs, respectively, that are serviced by a_f . Also $N_{a_f}^{a_f} \triangleq |\mathcal{U}_f(a_f)|$ and $N_{a_f}^{b_m} \triangleq |\mathcal{U}_m(a_f)|$. Finally, $\mathcal{U}_m(b_m)$ denotes the set of MUs serviced by the MBS b_m . Clearly, $\mathcal{U}_m = \cup_{a \in \mathcal{A}_f \cup \{b_m\}} \mathcal{U}_m(a)$. The number of MUs covered by the MBS b_m is denoted by $N_m^{b_m}$, i.e., $N_m^{b_m} \triangleq |\mathcal{U}_m(b_m)|$. Note that, by definition, $N_m = N_m^{b_m} + \sum_{a_f \in \mathcal{A}_f} N_{a_f}^{a_f}$.

C. Access policy and backhaul constraint

We consider the open access scenario with access parameter $\kappa \in [0, 1]$, studied in [2] for downlink communications and in [15] for uplink transmission, when the FAPs have no backhaul constraints. Let $d(u_m, a)$ denote the Euclidean distance between the (femto or macro) access point a and u_m . Then, in this access model an MU is served by its nearest FAP a_f if $\frac{d(u_m, a_f)}{d(u_m, b_m)}$ is less than κ and the backhaul constraint is not violated; otherwise it is served by the MBS.

To model the backhaul constraints, we assume that each FAP has access to a fixed broadband capacity, which translates into covering at most n_c users. The priority is always given to FUs. Once all FUs are serviced, if there is some remaining

unused capacity, it can be allocated to MUs. MU u_m is potentially assigned to FAP a_f , if $d(u_m, a_f) \leq \kappa d(u_m, b_m)$. If there are more than one FAPs satisfying this condition, u_m considers only the closest one. From all potential MUs of an FAP a_f with $N_{a_f}^{a_f}$ FUs, a_f randomly chooses up to $n_c - N_{a_f}^{a_f}$ of them to serve. It is reasonable to assume that $n_c \geq \bar{n}_{fu}$, or in other words, the capacity of each FAP is at least as large as the expected number of FUs in that cell.

In this model, due to the backhaul constraint, an MU can get arbitrarily close to an FAP a_f , and yet be serviced by the MBS. To avoid the arbitrarily large interference caused by such cases, we assume that, for any MU u_m , the ratio between its distances from any FAP a_f and the MBS, i.e., $d(u_m, a_f)/d(u_m, b_m)$, cannot be smaller than some threshold κ_o , where $\kappa_o \ll \kappa$. As argued in [15], this means that for an FAP a_f located at distance d from b_m , there exists a circle of radius $\frac{\kappa_o}{1-\kappa_o}d$ that includes a_f , where no MUs are allowed. In general, we can assume that κ_o depends on d , and as a special case tune it such that the excluded circle of all FAPs have the same radius. While our analysis can be generalized to this case in a straightforward manner, to simplify the statement of the results, we assume that κ_o is fixed for all FAPs.

D. Channel Model

To model the channel between user u and access point a , $a \in \{b_m, a_f\}$, both small scale fading and path loss are considered. So it is assumed that the fading coefficients corresponding to the channel in subband $i \in [1 : n_s]$ from user u to a , $H_{u,a}^i$, follows the Rayleigh distribution with parameter σ^2 . Furthermore, we assume that the coefficients corresponding to different subbands and also different channels are all independent. The path loss is modeled as $PL_{u,a} = L_0 d_{u,a}^\alpha$, where L_0 is the path loss at unit distance, and $\alpha > 2$ denotes the attenuation factor [3].

In this paper, we assume that every user employs power control to compensate for the effect of path loss. By power control, MUs serviced by the MBS intend to achieve a received power level of p_m , and FUs and MUs serviced by FAPs adjust their transmitted powers to achieve a received power of p_f .

III. USERS DENSITY DISTRIBUTION

In this section, we study the distributions of the random variables $N_{a_f}^{a_f}$, $N_{a_f}^{b_m}$, $N_m^{b_m}$ and N_m . As argued in [15], given FAP a_f at distance r from b_m , the set of points satisfying $d(u_m, a_f) \leq \kappa d(u_m, b_m)$ is the set of points inside a circle of radius $r_c = (\frac{\kappa}{1-\kappa^2})r$. (Refer to Fig. 1.) The distance between the center of this circle and b_m is equal to $\frac{r}{1-\kappa^2}$. For $\kappa \in (0, 1)$, $\frac{\kappa}{1-\kappa^2}$ is an increasing function of κ , which implies that increasing κ translates into increasing the coverage area of an

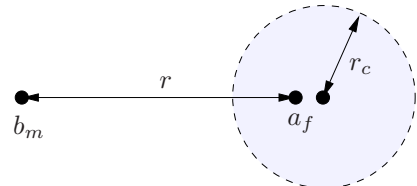


Fig. 1. MUs served by a_f located at distance r from b_m .

FAP. As a special case, when $\kappa = 0$, the FAP only covers FUs, and hence has a closed access policy.

For MUs serviced by FAPs, the potential coverage area of FAP a_f located at distance d from b_m is a circle of radius $(\frac{\kappa}{1-\kappa^2})d$. Let $\mathcal{U}_m(a_f)$ denote the MUs that fall in the coverage area of FAP a_f . Due to the backhaul constraint, not all the MUs falling in $\mathcal{U}_m(a_f)$ can be serviced by a_f . Therefore, they can be partitioned into two groups, $\mathcal{U}_m^s(a_f)$ and $\mathcal{U}_m^{ns}(a_f)$, representing the MUs that are serviced by a_f and the MUs that fall in the coverage area of a_f , but are serviced by b_m , respectively. Let $N_{m,s}^{a_f} \triangleq |\mathcal{U}_m^s(a_f)|$ and $N_{m,ns}^{a_f} \triangleq |\mathcal{U}_m^{ns}(a_f)|$. Stochastically,

$$N_{m,s}^{a_f} = \min(N_1, (n_c - N_2)^+),$$

and

$$N_{m,ns}^{a_f} = N_1 - N_{m,s}^{a_f} = (N_1 - (n_c - N_2)^+)^+,$$

where N_1 and N_2 are independent and distributed as $\text{Pois}(\bar{n}_{\text{mu}}^d)$ with

$$\bar{n}_{\text{mu}}^d \triangleq \pi \mu_m \left(\left(\frac{\kappa}{1-\kappa^2} \right)^2 - \left(\frac{\kappa_o}{1-\kappa_o^2} \right)^2 \right) d^2 \quad (1)$$

and $\text{Pois}(\bar{n}_{\text{fu}})$, respectively.

Lemma 1. *The Laplace transform of $N_{m,ns}^{a_f}$, the number of MUs that fall in the coverage area of FAP a_f located at distance d from the MBS b_m but serviced by b_m , satisfies*

$$\Phi_{N_{m,ns}^{a_f}}(s|d_f) \leq 1 - \mathcal{P}(n_c, \bar{n}_{\text{fu}}) + e^{\bar{n}_{\text{mu}}^d(e^{-s}-1)} \mathcal{P}(n_c, \bar{n}_{\text{fu}}).$$

Proof: By definition, the number of MUs in $\mathcal{U}_m^{ns}(a_f)$ can be written as $|\mathcal{U}_m^{ns}(a_f)| = N_1 - |\mathcal{U}_m^s(a_f)| = (N_1 - (n_c - N_2)^+)^+$, where N_1 and N_2 are independent and distributed as $\text{Pois}(\bar{n}_{\text{mu}}^d)$ and $\text{Pois}(\bar{n}_{\text{fu}})$, respectively. Therefore,

$$\begin{aligned} \Phi_{|\mathcal{U}_m^{ns}(a_f)|}(s|d_f) &= \mathbb{E} \left[e^{-s|\mathcal{U}_m^{ns}(a_f)|} | N_2 < n_c \right] \mathbb{P}(N_2 < n_c) \\ &\quad + \mathbb{E} \left[e^{-s|\mathcal{U}_m^{ns}(a_f)|} | N_2 \geq n_c \right] \mathbb{P}(N_2 \geq n_c) \\ &= \mathbb{E} \left[e^{-s|\mathcal{U}_m^{ns}(a_f)|} | N_2 < n_c \right] \mathbb{P}(N_2 < n_c) \\ &\quad + \mathbb{E} \left[e^{-sN_1} \right] \mathbb{P}(N_2 \geq n_c), \end{aligned} \quad (2)$$

where the last line follows from the independence of N_1 and N_2 . Since $\mathbb{E}[e^{-s|\mathcal{U}_m^{ns}(a_f)|} | N_2 < n_c] \leq 1$, from (2),

$$\begin{aligned} \Phi_{|\mathcal{U}_m^{ns}(a_f)|}(s|d_f) &\leq \mathbb{P}(N_2 < n_c) + \mathbb{E} \left[e^{-sN_1} \right] \mathbb{P}(N_2 \geq n_c) \\ &= 1 - \mathcal{P}(n_c, \bar{n}_{\text{fu}}) + e^{\bar{n}_{\text{mu}}^d(e^{-s}-1)} \mathcal{P}(n_c, \bar{n}_{\text{fu}}). \end{aligned}$$

Lemma 2. *Let $\gamma = (\frac{\kappa}{1-\kappa^2})^2 - (\frac{\kappa_o}{1-\kappa_o^2})^2$, and $\beta \triangleq \mathcal{P}(n_c, \bar{n}_{\text{fu}}) + (1 - \mathcal{P}(n_c, \bar{n}_{\text{fu}}))(\frac{e^{(\bar{n}_{\text{mu}}^d-1)\gamma\bar{n}_{\text{mu}}}-1}{(e^s-1)\gamma\bar{n}_{\text{bm}}})$. The Laplace transform of $N_m^{b_m}$, $\Phi_{N_m^{b_m}}(s)$, satisfies the following lower and upper bounds:*

$$\Phi_{N_m^{b_m}}(s) \geq e^{(e^{-s}-1)\bar{n}_{\text{mu}}},$$

and

$$\Phi_{N_m^{b_m}}(s) \leq e^{(e^{-s}-1)\bar{n}_{\text{mu}} + (\beta-1)\bar{n}_{\text{fap}}}.$$

Proof: To derive the lower bound, note that $N_m^{b_m} \leq N_m$, and therefore, for $s \geq 0$, $e^{-sN_m^{b_m}} \geq e^{-sN_m}$. Hence,

$$\mathbb{E}[e^{-sN_m^{b_m}}] \geq \mathbb{E}[e^{-sN_m}] = e^{\bar{n}_{\text{mu}}(e^{-s}-1)}.$$

Let $N_{\text{fap}} \triangleq |\mathcal{A}_f|$. Each FAP $a_f \in \mathcal{A}_f$, at most, covers $\min(N_1^{a_f}, (n_c - N_2^{a_f})^+)$ MUs, where $N_1^{a_f} \sim \text{Pois}(\bar{n}_{\text{mu}}^{d(a_f, b_m)})$ and $N_2^{a_f} \sim \text{Pois}(\bar{n}_{\text{fu}})$, where \bar{n}_{mu}^d is defined in (1). Let $N^{a_f} \triangleq \min(N_1^{a_f}, (n_c - N_2^{a_f})^+)$. Conditioned on \mathcal{A}_f , $\{N^{a_f}\}_{a_f \in \mathcal{A}_f}$ are independent and identically distributed (i.i.d.) random variables. Then, $N_m^{b_m} \geq N_m - \sum_{a_f \in \mathcal{A}_f} N^{a_f}$. Therefore,

$$\begin{aligned} \Phi_{N_m^{b_m}}(s) &= \mathbb{E}[e^{-sN_m^{b_m}}] \\ &\leq \mathbb{E}[e^{-sN_m}] \mathbb{E}[e^{s \sum_{a_f \in \mathcal{A}_f} N^{a_f}}] \\ &= \mathbb{E}[e^{-sN_m}] \mathbb{E} \left[\mathbb{E} \left[\prod_{a_f \in \mathcal{A}_f} e^{sN^{a_f}} | \mathcal{A}_f \right] \right] \\ &\stackrel{(a)}{=} \mathbb{E}[e^{-sN_m}] \mathbb{E}[(\mathbb{E}[e^{sN^{a_f}}])^{N_{\text{fap}}}] \\ &= e^{(e^{-s}-1)\bar{n}_{\text{mu}}} e^{\bar{n}_{\text{fap}}(\mathbb{E}[e^{sN^{a_f}}]-1)}, \end{aligned} \quad (3)$$

where (a) follows because conditioned on $N_{\text{fap}} = i$, $\{N^{a_f}\}_{a_f \in \mathcal{A}_f}$ are i i.i.d. random variables. On the other hand,

$$\begin{aligned} \mathbb{E}[e^{sN^{a_f}}] &= \mathbb{E}[\mathbb{E}[e^{sN^{a_f}} | \mathbb{1}_{N_2^{a_f} \geq n_c}]] \\ &= \mathcal{P}(n_c, \bar{n}_{\text{fu}}) + \mathbb{E}[e^{sN^{a_f}} | N_2^{a_f} < n_c] (1 - \mathcal{P}(n_c, \bar{n}_{\text{fu}})) \\ &\stackrel{(a)}{\leq} \mathcal{P}(n_c, \bar{n}_{\text{fu}}) + \mathbb{E}[e^{sN_1^{a_f}} | N_2^{a_f} < n_c] (1 - \mathcal{P}(n_c, \bar{n}_{\text{fu}})) \\ &\stackrel{(b)}{=} \mathcal{P}(n_c, \bar{n}_{\text{fu}}) + \mathbb{E}[e^{sN_1^{a_f}}] (1 - \mathcal{P}(n_c, \bar{n}_{\text{fu}})), \end{aligned}$$

where (a) holds because $N^{a_f} \leq N_1^{a_f}$ and $s \geq 0$, and (b) follows from the independence of $N_1^{a_f}$ and $N_2^{a_f}$. Also,

$$\mathbb{E}[e^{sN_1^{a_f}}] = \mathbb{E}[\mathbb{E}[e^{sN_1^{a_f}} | d(a_f, b_m)]] = \mathbb{E}[e^{(e^s-1)\bar{n}_{\text{mu}}^{d(a_f, b_m)}}],$$

where \bar{n}_{mu}^d is defined in (1). But,

$$\mathbb{E}[e^{cd^2(a_f, b_m)}] = \int_0^R \frac{2r}{R^2} e^{cr^2} dr = \frac{e^{cR^2} - 1}{cR^2}. \quad (4)$$

Therefore,

$$\mathbb{E}[e^{sN^{a_f}}] \leq \mathcal{P}(n_c, \bar{n}_{\text{fu}}) + (1 - \mathcal{P}(n_c, \bar{n}_{\text{fu}})) \left(\frac{e^{(e^s-1)\gamma\bar{n}_{\text{mu}}}-1}{(e^s-1)\gamma\bar{n}_{\text{bm}}} \right). \quad (5)$$

Combining (3) and (5) yields the desired upper bound. ■

IV. MU SERVED BY AN FAP

In this section, we analyze the outage performance of an MU serviced by an FAP, in the described uplink network with backhaul constraints. We assume that the performance of the users is primarily limited by the interference caused by the other users of both tiers, and therefore ignore the effect of additive Gaussian noise (AWGN) in our analysis.

Consider FAP $a_f \in \mathcal{A}_f$ at distance d from MBS b_m , i.e., $d(a_f, b_m) = d$. Given the power control assumption, the upload SIR experienced by user $u_m \in \mathcal{U}_m(a_f)$ in subband $i \in \{1, 2, \dots, n_s\}$ is equal to

$$\text{SIR}_{m,f} = \frac{p_f |H_{u_m, a_f}^i|^2}{n_s I_{m,f}}, \quad (6)$$

where

$$\begin{aligned}
I_{m,f} = & \sum_{u_f \in \mathcal{U}_f(a_f)} \frac{p_f |H_{u_f,a_f}^i|^2}{g} + \sum_{\hat{u}_m \in \mathcal{U}_m(a_f) \setminus u_m} \frac{p_f |H_{\hat{u}_m,a_f}^i|^2}{g} \\
& + \sum_{\hat{a}_f \in \mathcal{A}_f \setminus a_f} \sum_{u \in \mathcal{U}_m(\hat{a}_f) \cup \mathcal{U}_f(\hat{a}_f)} \left(\frac{d(u, \hat{a}_f)}{d(u, a_f)} \right)^\alpha \frac{p_f |H_{u,\hat{a}_f}^i|^2}{g} \\
& + \sum_{\hat{u}_m \in \mathcal{U}_m(b_m)} \left(\frac{d(\hat{u}_m, b_m)}{d(\hat{u}_m, a_f)} \right)^\alpha \frac{p_m |H_{\hat{u}_m,a_f}^i|^2}{g}. \quad (7)
\end{aligned}$$

In (7), from left to right, the interference terms correspond to the interference caused by the FUs of FAP a_f , the other MUs of FAP a_f , users of the other FAPs and the MUs serviced by the MBS, respectively. Given FAP $\hat{a}_f \in \mathcal{A}_f \setminus a_f$, and (femto or macro) user $u \in \mathcal{U}_m(\hat{a}_f) \cup \mathcal{U}_f(\hat{a}_f)$ covered by \hat{a}_f , typically $d(u, \hat{a}_f) \ll d(u, a_f)$, or $\frac{d(u, \hat{a}_f)}{d(u, a_f)} \ll 1$. Therefore, unless the density of FAPs is very high, the effect of the interference caused by the users of other FAPs is negligible. Under this approximation, we have

$$I_{m,f} = \sum_{u \in \mathcal{U}_f(a_f) \cup \mathcal{U}_m(a_f) \setminus u_m} \frac{p_f |H_{u,a_f}^i|^2}{g} + \sum_{\hat{u}_m \in \mathcal{U}_m(b_m)} (\delta_{\hat{u}_m})^\alpha \frac{p_m |H_{\hat{u}_m,a_f}^i|^2}{g}, \quad (8)$$

where

$$\delta_{\hat{u}_m} \triangleq \frac{d(\hat{u}_m, b_m)}{d(\hat{u}_m, a_f)}. \quad (9)$$

Define the event $\mathcal{E} = \{d(a_f, b_m) = d, N_m^{a_f} \geq 1\}$. Then MU $u_m \in \mathcal{U}_m(a_f)$ is said to experience outage in subband i if $\text{SIR}_{m,f}$ is less than some pre-determined threshold θ . Therefore, the corresponding outage probability $P_{\text{out}}^{m,f}$ of MU u_m serviced by FAP a_f is defined as $P_{\text{out}}^{m,f}(\theta, d_f) = \text{P}(\text{SIR}_{m,f} < \theta | \mathcal{E})$, where $\text{SIR}_{m,f}$ is defined in (6). Since $|H_{u_m,a_f}^i|^2$ has an exponential distribution and is independent of other relevant random variables, it follows that

$$P_{\text{out}}^{m,f}(\theta, d_f) = 1 - \text{E}[e^{-(\frac{\theta n_g}{\sigma^2 p_f}) I_{m,f}} | \mathcal{E}]. \quad (10)$$

In the following two sections, we derive analytical upper and lower bounds on $P_{\text{out}}^{m,f}$.

Before stating the bounds, given FAP a_f at distance d_f from b_m , consider partitioning the coverage area \mathcal{S}_m of the MBS b_m , as described in Appendix A, into $2(t+1)$ regions. To perform this partitioning parameters $(\kappa_0, \dots, \kappa_t)$ are selected such that $\kappa_0 = \kappa < \kappa_1 < \kappa_2 < \dots < \kappa_t = 1$. For user u with δ_u defined in (9), $\hat{\delta}_u^{\text{ub}}$ and $\hat{\delta}_u^{\text{lb}}$ are defined as follows: $\hat{\delta}_u^{\text{ub}} = \kappa_i^{-1}$ and $\hat{\delta}_u^{\text{lb}} = \kappa_{i+1}^{-1}$, if $\kappa_{i+1} < \delta_u \leq \kappa_i^{-1}$, for $i = 0, \dots, t-1$; $\hat{\delta}_u^{\text{ub}} = \kappa_{i+1}$ and $\hat{\delta}_u^{\text{lb}} = \kappa_i$, if $\kappa_i < \delta_u \leq \kappa_{i+1}$, for $i = 0, \dots, t-1$; and $\hat{\delta}_u^{\text{ub}} = \kappa$ and $\hat{\delta}_u^{\text{lb}} = 0$, if $\delta_u \leq \kappa$. Note that by construction, unlike δ_u , $\hat{\delta}_u^{\text{lb}}$ and $\hat{\delta}_u^{\text{ub}}$ are discrete random variables. For all u and a_f , $\hat{\delta}_u^{\text{lb}} \leq \delta_u \leq \hat{\delta}_u^{\text{ub}}$.

A. Upper Bound on the Outage Probability $P_{\text{out}}^{m,f}$

For $i = 1, \dots, t$, and $\hat{u}_m \in \mathcal{U}_m \setminus \mathcal{U}_m(a_f)$, let

$$p_i = \text{P}(\hat{\delta}_{\hat{u}_m}^{\text{ub}} = \frac{1}{\kappa_{i-1}}) = \text{P}(\hat{\delta}_{\hat{u}_m}^{\text{lb}} = \frac{1}{\kappa_i}),$$

$$p_{-i} = \text{P}(\hat{\delta}_{\hat{u}_m}^{\text{ub}} = \kappa_i) = \text{P}(\hat{\delta}_{\hat{u}_m}^{\text{lb}} = \kappa_{i-1}),$$

and

$$p_0 = \text{P}(\hat{\delta}_{\hat{u}_m}^{\text{ub}} = \kappa_0) = \text{P}(\hat{\delta}_{\hat{u}_m}^{\text{lb}} = 0).$$

Also, let $\eta \triangleq \frac{p_f}{p_m}$, $\bar{n}_{m,d} \triangleq \pi(R^2 - (\frac{\kappa}{1-\kappa^2})^2 d^2) \mu_m$ and

$$q_1(\theta, d) \triangleq \sum_{i=1}^t \left(\frac{p_i}{1 + \frac{\theta}{n_h \eta \kappa_{i-1}^\alpha}} + \frac{p_{-i}}{1 + \frac{\theta \kappa_i^\alpha}{n_h \eta}} \right) + \frac{p_0}{1 + \frac{\theta \kappa_0^\alpha}{n_h \eta}}.$$

Theorem 1. The outage probability of an MU serviced by an FAP located at distance d from MBS, $P_{\text{out}}^{m,f}(\theta, d)$, is upper bounded by

$$1 - \left(\frac{1}{1 + \frac{\theta}{n_h}} \right)^{n_c-1} e^{\bar{n}_{m,d}(q_1(\theta, d)-1)} \Phi_{|\mathcal{U}_m^{\text{ns}}(a_f)|} \left(\log \left(1 + \frac{\theta}{\eta n_h \kappa_0^\alpha} \right) \right),$$

where $\Phi_{|\mathcal{U}_m^{\text{ns}}(a_f)|}$, the Laplace transform of $|\mathcal{U}_m^{\text{ns}}(a_f)|$, is derived in Appendix III.

Proof: For MUs serviced by FAPs, as discussed in [15], the potential coverage area of FAP a_f located at distance d from b_m is a circle of radius $(\frac{\kappa}{1-\kappa^2})d$. Due to the backhaul constraint, all the MUs falling in this circle, $\mathcal{U}_m(a_f)$, are not serviced by a_f . Users in $\mathcal{U}_m(a_f)$ can be partitioned into two groups, $\mathcal{U}_m^s(a_f)$ and $\mathcal{U}_m^{\text{ns}}(a_f)$, representing the MUs that are serviced by a_f and the MUs that fall in the coverage area of a_f , but are serviced by b_m , respectively.

Given the backhaul constraint of n_c users, there are at most $n_c - 1$ users (macro and femto) serviced by a_f that interfere with an FU covered by a_f . That is, $|\mathcal{U}_f(a_f) \cup \mathcal{U}_m^s(a_f) \setminus u_m| \leq n_c - 1$. Also, we always have $\mathcal{U}_m(b_m) \subseteq \mathcal{U}_m \setminus \mathcal{U}_m^s(a_f)$. Therefore, from (7),

$$\begin{aligned}
I_{m,f} & \leq \sum_{\ell=1}^{n_c-1} \frac{p_f}{g} |H_\ell|^2 + \sum_{\hat{u}_m \in \mathcal{U}_m \setminus \mathcal{U}_m^s(a_f)} \frac{(p_m \delta_{\hat{u}_m})^\alpha}{g} |H_{\hat{u}_m,a_f}^i|^2 \\
& = \sum_{\ell=1}^{n_c-1} \frac{p_f}{g} |H_\ell|^2 + \sum_{\hat{u}_m \in \mathcal{U}_m \setminus \mathcal{U}_m(a_f)} \frac{p_m (\delta_{\hat{u}_m})^\alpha}{g} |H_{\hat{u}_m,a_f}^i|^2 \\
& \quad + \sum_{\hat{u}_m \in \mathcal{U}_m^{\text{ns}}(a_f)} \frac{p_m (\delta_{\hat{u}_m})^\alpha}{g} |H_{\hat{u}_m,a_f}^i|^2 \\
& \stackrel{(a)}{\leq} \sum_{\ell=1}^{n_c-1} \frac{p_f}{g} |H_\ell|^2 + \sum_{\hat{u}_m \in \mathcal{U}_m \setminus \mathcal{U}_m(a_f)} (\delta_{\hat{u}_m})^\alpha \frac{p_m}{g} |H_{\hat{u}_m,a_f}^i|^2 \\
& \quad + \sum_{\hat{u}_m \in \mathcal{U}_m^{\text{ns}}(a_f)} \frac{p_m}{\kappa_0^\alpha g} |H_{\hat{u}_m,a_f}^i|^2 \\
& \stackrel{(b)}{\leq} \sum_{\ell=1}^{n_c-1} \frac{p_f}{g} |H_\ell|^2 + \sum_{\hat{u}_m \in \mathcal{U}_m \setminus \mathcal{U}_m(a_f)} \frac{p_m (\hat{\delta}_{\hat{u}_m}^{\text{ub}})^\alpha}{g} |H_{\hat{u}_m,a_f}^i|^2 \\
& \quad + \sum_{\hat{u}_m \in \mathcal{U}_m^{\text{ns}}(a_f)} \frac{p_m}{\kappa_0^\alpha g} |H_{\hat{u}_m,a_f}^i|^2, \quad (11)
\end{aligned}$$

where $\{|H_\ell|^2 : \ell = 1, \dots, n_c-1\}$ are i.i.d. exponential random variables independent of other random variables in (11). Also, (a) holds because by assumption, $d(\hat{u}_m, b_m)/d(\hat{u}_m, \hat{a}_f) \leq \kappa_0^{-1}$, for all $\hat{u}_m \in \mathcal{U}_m$, and all $\hat{a}_f \in \mathcal{A}_f$, and (b) follows because $\delta_u \leq \hat{\delta}_u^{\text{ub}}$.

Since the MUs in \mathcal{U}_m are generated according to a PPP and the users in $\mathcal{U}_m \setminus \mathcal{U}_m(a_f)$ and $\mathcal{U}_m^{\text{ns}}(a_f)$ have non-overlapping supports, they are independent. Therefore, combining (10) and

(11), it follows that

$$\begin{aligned}
P_{\text{out}}^{m,f} &= 1 - \mathbb{E}[e^{-(\frac{\theta n_s}{\sigma^2 p_f}) I_{m,f}} | \mathcal{E}] \\
&\leq 1 - \left(\frac{1}{1 + \frac{\theta}{n_h}} \right)^{n_c - 1} \\
&\quad \times \mathbb{E} \left[\left(\mathbb{E} \left[e^{-\frac{\theta}{n_h \eta \sigma^2} (\delta_{\hat{u}_m}^{\text{ub}})^\alpha |H_{\hat{u}_m, a_f}^i|^2} \right] \right)^{|U_m| - |U_m(a_f)|} \right] \\
&\quad \times \mathbb{E} \left[\left(\frac{1}{1 + \frac{\theta}{\eta n_h \kappa_o^\alpha}} \right)^{|U_m^{\text{ns}}(a_f)|} \right]. \quad (12)
\end{aligned}$$

Since $\delta_{\hat{u}_m}^{\text{ub}}$ and $|H_{\hat{u}_m, a_f}^i|$ are independent,

$$\mathbb{E} \left[e^{-\frac{\theta}{n_h \eta \sigma^2} (\delta_{\hat{u}_m}^{\text{ub}})^\alpha |H_{\hat{u}_m, a_f}^i|^2} \right] = q_1(\theta, d). \quad (13)$$

Finally, $|U_m| - |U_m(a_f)|$ is a Poisson random variable of mean $\bar{n}_{m,d}$. Therefore, combining (12) and (13) yields the desired result. ■

B. Lower Bound on the Outage Probability $P_{\text{out}}^{m,f}$

Consider partitioning the MUs in $U_m(b_m) \setminus U_m^{\text{ns}}(a_f)$ into two groups:

- i) $U_m^{\text{in}}(b_m)$: the subset of MUs that fall into the coverage area of at least one FAP in $\mathcal{A}_f \setminus a_f$, but are serviced by the MBS due to the backhaul constraints, i.e.,

$$U_m^{\text{in}}(b_m) \triangleq \cup_{\hat{a}_f \in \mathcal{A}_f \setminus a_f} U_m^{\text{ns}}(\hat{a}_f),$$

- ii) $U_m^{\text{out}}(b_m)$: the subset of MUs that are serviced by the MBS because they do not fall into the coverage area of any FAP, i.e.,

$$U_m^{\text{out}}(b_m) \triangleq U_m(b_m) \setminus (U_m^{\text{in}}(b_m) \cup U_m^{\text{ns}}(a_f)).$$

For $i = 1, \dots, t$, and $\hat{u}_m \in U_m^{\text{out}}(b_m)$, let

$$p'_i = \mathbb{P}(\hat{\delta}_{\hat{u}_m}^{\text{ub}} = \frac{1}{\kappa_{i-1}}) = \mathbb{P}(\hat{\delta}_{\hat{u}_m}^{\text{lb}} = \frac{1}{\kappa_i}),$$

$$p'_{-i} = \mathbb{P}(\hat{\delta}_{\hat{u}_m}^{\text{ub}} = \kappa_i) = \mathbb{P}(\hat{\delta}_{\hat{u}_m}^{\text{lb}} = \kappa_{i-1}),$$

and $p'_0 = \mathbb{P}(\hat{\delta}_{\hat{u}_m}^{\text{ub}} = \kappa_0) = \mathbb{P}(\hat{\delta}_{\hat{u}_m}^{\text{lb}} = 0)$. Now define

$$q_2(\theta, d) \triangleq p'_0 + \sum_{i=1}^t \left(\frac{p'_i}{1 + \frac{\theta}{n_h \eta \kappa_i^\alpha}} + \frac{p'_{-i}}{1 + \frac{\theta}{n_h \eta \kappa_{i-1}^\alpha}} \right), \quad (14)$$

$\gamma_1 \triangleq \pi(1 - q_2(\theta, d))(\frac{\kappa}{1 - \kappa^2})^2 \mu_m$, $\gamma_2 \triangleq \frac{\theta}{\eta n_h (1 + \kappa)^\alpha}$, and $\gamma_3 \triangleq \pi \mu_m ((\frac{\kappa}{1 - \kappa^2})^2 - (\frac{\kappa_o}{1 - \kappa_o^2})^2)$. Consider FAP a_f at distance d from MBS b_m and FAP $\hat{a}_f \in \mathcal{A}_f \setminus a_f$. Let $(D_1, D_2) = (d(\hat{a}_f, b_m), d(\hat{a}_f, a_f))$, and define

$$\gamma_4 \triangleq \mathbb{E} \left[e^{D_1^2(\gamma_1 - \frac{\gamma_2 \gamma_3 D_1^\alpha}{D_2^2 + \gamma_2 D_1^\alpha})} \right]. \quad (15)$$

Note that γ_4 can easily be computed through Monte Carlo simulations.

Theorem 2. Let

$$\chi \triangleq \left(\frac{1 - e^{-\gamma_1 R^2}}{\gamma_1 R^2} \right) (1 - \mathcal{P}(n_c, \bar{n}_{\text{fu}})) + \gamma_4 \mathcal{P}(n_c, \bar{n}_{\text{fu}}).$$

Then, $P_{\text{out}}^{m,f}(\theta, d)$, the outage probability of an MU serviced by an FAP located at distance d from the MBS, is lower bounded

by

$$\begin{aligned}
&1 - e^{-\bar{n}_{\text{mu}}(1 - q_2)} \frac{e^{\bar{n}_{\text{fap}}(\chi - 1)} - e^{-\bar{n}_{\text{fap}}}}{(1 - e^{-\bar{n}_{\text{fap}}})\chi} \\
&\quad \times \Phi_{|U_m^{\text{ns}}(a_f)|} \left(\log \left(1 + \frac{\theta}{\eta n_h \kappa^\alpha} \right) \right) (1 + O(\kappa^\alpha)), \quad (16)
\end{aligned}$$

where $\Phi_{|U_m^{\text{ns}}(a_f)|}$ is computed in Section III.

Proof: Considering the described partitioning of users in $U_m(b_m) \setminus U_m^{\text{ns}}(a_f)$, and ignoring the interference caused by the other FUs and MUs that are serviced by a_f , $I_{m,f}$ can be lower bounded as

$$\begin{aligned}
I_{m,f} &\geq \sum_{\hat{u}_m \in U_m^{\text{in}}(b_m)} \frac{p_m}{g} (\delta_{\hat{u}_m})^\alpha |H_{\hat{u}_m, a_f}^i|^2 \\
&\quad + \sum_{\hat{u}_m \in U_m^{\text{out}}(b_m)} \frac{p_m}{g} (\delta_{\hat{u}_m})^\alpha |H_{\hat{u}_m, a_f}^i|^2 \\
&\quad + \sum_{\hat{u}_m \in U_m^{\text{ns}}(a_f)} \frac{p_m}{g} (\delta_{\hat{u}_m})^\alpha |H_{\hat{u}_m, a_f}^i|^2. \quad (17)
\end{aligned}$$

For users in $U_m^{\text{in}}(b_m)$, consider FAP $\hat{a}_f \in \mathcal{A}_f \setminus a_f$, and user $\hat{u}_m \in U_m^{\text{ns}}(\hat{a}_f)$. (Refer to Fig. 2.) Let $d_o = d(\hat{a}_f, b_m)$. If FAP a_f does not fall into the coverage area of \hat{a}_f , as shown in Fig. 2, $d(\hat{u}_m, b_m) \geq \frac{1}{1 - \kappa^2} d_o - \frac{\kappa}{1 - \kappa^2} d_o = \frac{d_o}{1 + \kappa}$ and $d(\hat{u}_m, a_f) \leq d(\hat{c}_f, a_f) + \frac{\kappa}{1 - \kappa^2} d_o$, where \hat{c}_f denotes the center of the coverage area of \hat{a}_f . Hence,

$$\frac{d(\hat{u}_m, b_m)}{d(\hat{u}_m, a_f)} \geq \frac{\frac{1}{1 + \kappa} d(\hat{a}_f, b_m)}{d(\hat{c}_f, a_f) + \frac{\kappa}{1 - \kappa^2} d(\hat{a}_f, b_m)}. \quad (18)$$

On the other hand, since both \hat{a}_f and \hat{u}_m are located in a circle of radius $\frac{\kappa}{1 - \kappa^2} d_o$, $d(\hat{a}_f, \hat{u}_m) \leq \frac{2\kappa}{1 - \kappa^2} d_o$. Therefore $d(\hat{a}_f, \hat{u}_m) = O(\kappa)$, and

$$\frac{\frac{1}{1 + \kappa} d(\hat{a}_f, b_m)}{d(\hat{c}_f, a_f) + \frac{\kappa}{1 - \kappa^2} d(\hat{a}_f, b_m)} = \frac{d(\hat{a}_f, b_m)}{(1 + \kappa)d(\hat{a}_f, a_f)} + O(\kappa).$$

For users in $U_m^{\text{ns}}(a_f)$, $\frac{1}{\kappa} \leq \frac{d(\hat{u}_m, b_m)}{d(\hat{u}_m, a_f)} \leq \frac{1}{\kappa_o}$. Let $\delta_{\hat{a}_f} \triangleq \frac{d(\hat{a}_f, b_m)}{d(\hat{a}_f, a_f)}$. Then, noting that $\hat{\delta}_{\hat{u}_m}^{\text{lb}} \leq \delta_{\hat{u}_m}$, from (17), conditioned on the event that none of the other FAPs falls into the coverage area of a_f , it follows that

$$\begin{aligned}
I_{m,f} &\geq \sum_{\hat{u}_m \in U_m^{\text{ns}}(a_f)} \frac{p_m}{\kappa^\alpha g} |H_{\hat{u}_m, a_f}^i|^2 \\
&\quad + \sum_{\hat{a}_f \in \mathcal{A}_f \setminus a_f} \frac{p_m}{g(1 + \kappa)^\alpha} (\delta_{\hat{a}_f})^\alpha \sum_{\hat{u}_m \in U_m^{\text{ns}}(\hat{a}_f)} |H_{\hat{u}_m, a_f}^i|^2 \\
&\quad + \sum_{\hat{u}_m \in U_m^{\text{out}}(b_m)} \frac{(\hat{\delta}_{\hat{u}_m}^{\text{lb}})^\alpha p_m}{g} |H_{\hat{u}_m, a_f}^i|^2 + O(\kappa^\alpha). \quad (19)
\end{aligned}$$

All the interference terms in (19) have non-overlapping supports, and hence, conditioned on the locations of FAPs, are independent. Therefore, combining (10) and (19), it follows that

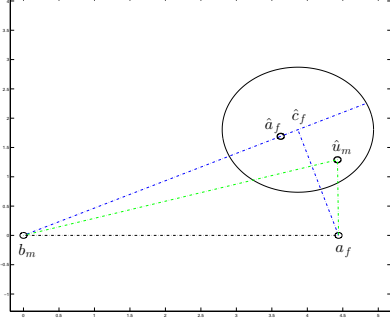


Fig. 2. User $\hat{u}_m \in \mathcal{U}_m^{\text{ns}}(\hat{a}_f)$.

$$\begin{aligned}
 P_{\text{out}}^{m,f} &= 1 - \mathbb{E}[e^{-\left(\frac{\theta n_s}{\sigma^2 p_f}\right) I_{m,f}} | \mathcal{A}_f, \mathcal{E}] \\
 &\geq 1 - \mathbb{E}\left[e^{-\frac{\theta}{\eta n_h \sigma^2 \kappa^\alpha} \sum_{\hat{u}_m \in \mathcal{U}_m^{\text{ns}}(a_f)} |H_{\hat{u}_m, a_f}^i|^2} \middle| \mathcal{E}\right] \\
 &\quad \times \mathbb{E}\left[\mathbb{E}\left[e^{-\frac{\theta}{\eta n_h \sigma^2} \sum_{\hat{u}_m \in \mathcal{U}_m^{\text{out}}(b_m)} (\delta_{\hat{u}_m}^{\text{lb}})^\alpha |H_{\hat{u}_m, a_f}^i|^2} \middle| \mathcal{E}, \mathcal{A}_f\right]\right] \\
 &\quad \times \mathbb{E}\left[e^{-\frac{\theta}{\eta n_h \sigma^2 (1+\kappa)^\alpha} \sum_{\hat{a}_f \in \mathcal{A}_f \setminus a_f} (\delta_{\hat{a}_f})^\alpha \sum_{\hat{u}_m \in \mathcal{U}_m^{\text{ns}}(\hat{a}_f)} |H_{\hat{u}_m, a_f}^i|^2} \middle| \mathcal{E}, \mathcal{A}_f\right] \\
 &\quad \times (1 + O(\kappa^\alpha)). \tag{20}
 \end{aligned}$$

Let S_{out} denote the area of the region that is not covered by any of the FAPs. Then, conditioned on $(\mathcal{E}, \mathcal{A}_f)$, $|\mathcal{U}_m^{\text{out}}(b_m)|$ is distributed as $\text{Pois}(S_{\text{out}}\mu_m)$. Therefore, as

$$\mathbb{E}\left[e^{-\frac{\theta}{\eta n_h \sigma^2} (\delta_{\hat{u}_m}^{\text{lb}})^\alpha |H_{\hat{u}_m, a_f}^i|^2} \middle| \hat{u}_m \in \mathcal{U}_m^{\text{out}}(b_m)\right] = q_2(\theta, d),$$

it follows that

$$\begin{aligned}
 &\mathbb{E}\left[e^{-\frac{\theta}{\eta n_h \sigma^2} \sum_{\hat{u}_m \in \mathcal{U}_m^{\text{out}}(b_m)} (\delta_{\hat{u}_m}^{\text{lb}})^\alpha |H_{\hat{u}_m, a_f}^i|^2} \middle| \mathcal{E}, \mathcal{A}_f\right] \\
 &= \mathbb{E}\left[\left(\mathbb{E}\left[e^{-\frac{\theta}{\eta n_h \sigma^2} (\delta_{\hat{u}_m}^{\text{lb}})^\alpha |H_{\hat{u}_m, a_f}^i|^2}\right]\right)^{|\mathcal{U}_m^{\text{out}}(b_m)|} \middle| \mathcal{E}, \mathcal{A}_f\right] \\
 &= e^{(q_2(\theta, d)-1)S_{\text{out}}\mu_m}. \tag{21}
 \end{aligned}$$

On the other hand,

$$\begin{aligned}
 &\mathbb{E}\left[e^{-\frac{\theta}{\eta n_h \sigma^2 (1+\kappa)^\alpha} \sum_{\hat{a}_f \in \mathcal{A}_f \setminus a_f} (\delta_{\hat{a}_f})^\alpha \sum_{\hat{u}_m \in \mathcal{U}_m^{\text{ns}}(\hat{a}_f)} |H_{\hat{u}_m, a_f}^i|^2} \middle| \mathcal{E}, \mathcal{A}_f\right] \\
 &= \prod_{\hat{a}_f \in \mathcal{A}_f \setminus a_f} \left(\frac{1}{1 + \gamma_2(\delta_{\hat{a}_f})^\alpha}\right)^{N_{m,n_c}^{\hat{a}_f}}. \tag{22}
 \end{aligned}$$

Combining (20), (21), and (22), and noting that $S_{\text{out}} \geq \pi R^2 - \pi(\frac{\kappa}{1-\kappa^2})^2 \sum_{\hat{a}_f \in \mathcal{A}_f \setminus a_f} d^2(a_f, b_m)$, we have

$$\begin{aligned}
 P_{\text{out}}^{m,f} &\geq 1 - e^{-\pi R^2 \mu_m (1-q_2)} \mathbb{E}\left[e^{-\frac{\theta}{\eta n_h \sigma^2 \kappa^\alpha} \sum_{\hat{u}_m \in \mathcal{U}_m^{\text{ns}}(a_f)} |H_{\hat{u}_m, a_f}^i|^2} \middle| \mathcal{E}\right] \\
 &\quad \times \mathbb{E}\left[\prod_{\hat{a}_f \in \mathcal{A}_f \setminus a_f} e^{\pi(1-q_2)(\frac{\kappa}{1-\kappa^2})^2 d^2(\hat{a}_f, b_m) \mu_m} \left(\frac{1}{1 + \gamma_2(\delta_{\hat{a}_f})^\alpha}\right)^{N_{m,n_c}^{\hat{a}_f}} \middle| \mathcal{E}\right] \\
 &= 1 - e^{-\bar{n}_{\text{mu}}(1-q_2)} \mathbb{E}\left[\left(\frac{1}{1 + \frac{\theta}{\eta n_h \kappa^\alpha}}\right)^{|\mathcal{U}_m^{\text{ns}}(a_f)|} \middle| \mathcal{E}\right] \\
 &\quad \times \mathbb{E}\left[\left(\mathbb{E}\left[e^{\gamma_1 d^2(\hat{a}_f, b_m)} \left(\frac{1}{1 + \gamma_2(\delta_{\hat{a}_f})^\alpha}\right)^{N_{m,n_c}^{\hat{a}_f}}\right]^{|\mathcal{A}_f|-1} \middle| \mathcal{E}\right]\right]. \tag{23}
 \end{aligned}$$

Let $(D_1, D_2) = (d(\hat{a}_f, b_m), d(\hat{a}_f, a_f))$. Employing the upper bound derived in Lemma 1, we have

$$\begin{aligned}
 &\mathbb{E}\left[e^{\gamma_1 D_1^2} \left(\frac{1}{1 + \gamma_2(\delta_{\hat{a}_f})^\alpha}\right)^{N_{m,n_c}^{\hat{a}_f}}\right] \\
 &= \mathbb{E}\left[\mathbb{E}\left[e^{\gamma_1 D_1^2} \left(\frac{1}{1 + \gamma_2(\delta_{\hat{a}_f})^\alpha}\right)^{N_{m,n_c}^{\hat{a}_f}} \middle| D_1, D_2\right]\right] \\
 &\leq (1 - \mathcal{P}(n_c, \bar{n}_{\text{fu}})) \mathbb{E}[e^{\gamma_1 D_1^2}] + \mathcal{P}(n_c, \bar{n}_{\text{fu}}) \mathbb{E}[e^{D_1^2(\gamma_1 - \frac{\gamma_2 \gamma_3 D_1^\alpha}{D_2^\alpha + \gamma_2 D_1^\alpha})}] \\
 &= \chi. \tag{24}
 \end{aligned}$$

Finally, combining (23) and (24) yields the desired result. ■

V. MU SERVED BY THE MBS

In this section, we analyze the outage performance of an MU serviced by the MBS. The upload SIR experienced by user $u_m \in \mathcal{U}_m(b_m)$ in subband $i \in \{1, 2, \dots, n_s\}$ is equal to

$$\text{SIR}_{m,m} = \frac{\frac{p_m |H_{u_m, b_m}^i|^2}{n_s}}{I_{m,m}}, \tag{25}$$

where

$$\begin{aligned}
 I_{m,m} &= \sum_{a_f \in \mathcal{A}_f} \sum_{u \in \mathcal{U}_m(a_f) \cup \mathcal{U}_f(a_f)} \left(\frac{d(u, a_f)}{d(u, b_m)}\right)^\alpha \frac{p_f |H_{u, a_f}^i|^2}{g} \\
 &\quad + \sum_{\hat{u}_m \in \mathcal{U}_m(b_m) \setminus u_m} \frac{p_m |H_{\hat{u}_m, b_m}^i|^2}{g}.
 \end{aligned}$$

According to the assumed access policy, for user $u \in \mathcal{U}_m(a_f)$, we have $d(u, a_f) \leq \kappa d(u, b_m)$, and therefore $(\frac{d(u, a_f)}{d(u, b_m)})^\alpha \leq \kappa^\alpha \ll 1$. Also, for user $u \in \mathcal{U}_f(a_f)$, it is reasonable to assume that $d(u, a_f) \ll d(u, b_m)$. Hence, the first interference term in (26) is negligible compared to the second one. Under this approximation,

$$I_{m,m} = \sum_{\hat{u}_m \in \mathcal{U}_m(b_m) \setminus u_m} \frac{p_m |H_{\hat{u}_m, b_m}^i|^2}{g}. \tag{26}$$

Theorem 3. Let $\bar{n}_o \triangleq \bar{n}_{b_m} (\frac{\kappa}{1-\kappa^2})^2$ and $\epsilon \triangleq e^{-\bar{n}_{b_m} + \bar{n}_{\text{fap}} (\frac{e^{\bar{n}_o} - 1}{\bar{n}_o} - 1)}$. The outage probability experienced by an MU serviced by the MBS, $P_{\text{out}}^{m,m}(\theta) = \mathbb{P}(\text{SIR}_{m,m} \leq \theta)$, satisfies

$$\begin{aligned}
 P_{\text{out}}^{m,m}(\theta) &\geq 1 - \frac{1 + \frac{\theta}{n_h}}{1 - \epsilon} \Phi_{N_m^{b_m}}(\ln(1 + \frac{\theta}{n_h})), \\
 P_{\text{out}}^{m,m}(\theta) &\leq 1 - (1 + \frac{\theta}{n_h})(\Phi_{N_m^{b_m}}(\ln(1 + \frac{\theta}{n_h})) - \epsilon).
 \end{aligned}$$

Proof: Combining (25) and (26), since $|H_{u_m, b_m}^i|^2$ satisfies an exponential distribution, we have

$$\begin{aligned}
 P_{\text{out}}^{m,m}(\theta) &= 1 - \mathbb{E}[e^{-(\frac{\theta n_s}{\sigma^2 p_m}) I_{m,m}}] \\
 &= 1 - \mathbb{E}\left[\left(\frac{1}{1 + \frac{\theta}{n_h}}\right)^{N_m^{b_m}-1} \middle| N_m^{b_m} \geq 1\right]. \tag{27}
 \end{aligned}$$

Let $a \triangleq \frac{1}{1 + \frac{\theta}{n_h}}$. Then,

$$\begin{aligned}
\mathbb{E} \left[\left(\frac{1}{1 + \frac{\theta}{n_h}} \right)^{N_m^{b_m}-1} \middle| N_m^{b_m} \geq 1 \right] &= \mathbb{E} [a^{N_m^{b_m}-1} | N_m^{b_m} \geq 1] \\
&= \sum_{i=1}^{\infty} a^{i-1} \mathbb{P}(N_m^{b_m} = i | N_m^{b_m} \geq 1) \\
&= \sum_{i=1}^{\infty} a^{i-1} \frac{\mathbb{P}(N_m^{b_m} = i)}{\mathbb{P}(N_m^{b_m} \geq 1)} \\
&= \frac{a^{-1} (\mathbb{E}[a^{N_m^{b_m}}] - \mathbb{P}(N_m^{b_m} = 0))}{1 - \mathbb{P}(N_m^{b_m} = 0)} \\
&= \frac{a^{-1} (\Phi_{N_m^{b_m}}(-\ln a) - \mathbb{P}(N_m^{b_m} = 0))}{1 - \mathbb{P}(N_m^{b_m} = 0)}.
\end{aligned}$$

We first derive an upper bound in $\mathbb{P}(N_m^{b_m} = 0)$. As defined in Section IV-B, let $\mathcal{U}_m^{\text{out}}(b_m)$ denote the set of users in $\mathcal{U}_m(b_m)$ that fall into the coverage area of no FAP. Also, let $\mathcal{U}_m^{\text{in}}(b_m) = \mathcal{U}_m(b_m) \setminus \mathcal{U}_m^{\text{out}}(b_m)$. Then,

$$\mathbb{P}(N_m^{b_m} = 0) = \mathbb{P}(|\mathcal{U}_m^{\text{out}}(b_m)| = |\mathcal{U}_m^{\text{in}}(b_m)| = 0) \leq \mathbb{P}(|\mathcal{U}_m^{\text{out}}(b_m)| = 0).$$

Conditioned on \mathcal{A}_f , $|\mathcal{U}_m^{\text{out}}(b_m)|$ is distributed as $\text{Pois}(S_{\text{out}}\mu_m)$. Therefore,

$$\mathbb{P}(|\mathcal{U}_m^{\text{out}}(b_m)| = 0) = \mathbb{E}[e^{-S_{\text{out}}\mu_m}].$$

But $S_{\text{out}} \geq \pi R^2 - \pi \left(\frac{\kappa}{1-\kappa^2} \right)^2 \sum_{a_f \in \mathcal{A}_f} d^2(a_f, b_m)$. Hence,

$$\begin{aligned}
\mathbb{P}(|\mathcal{U}_m^{\text{out}}(b_m)| = 0) &\leq \mathbb{E}[e^{-\bar{n}_{b_m} + \pi \left(\frac{\kappa}{1-\kappa^2} \right)^2 \mu_m \sum_{a_f \in \mathcal{A}_f} d^2(a_f, b_m)}] \\
&= e^{-\bar{n}_{b_m}} \mathbb{E} \left[\left(\mathbb{E}[e^{\pi \left(\frac{\kappa}{1-\kappa^2} \right)^2 d^2(a_f, b_m)}] \right)^{|\mathcal{A}_f|} \right] \\
&= e^{-\bar{n}_{b_m}} \mathbb{E} \left[\left(\frac{e^{\bar{n}_o} - 1}{\bar{n}_o} \right)^{|\mathcal{A}_f|} \right] \\
&= e^{-\bar{n}_{b_m} + \bar{n}_{\text{fap}} \left(\frac{e^{\bar{n}_o} - 1}{\bar{n}_o} - 1 \right)} \\
&= \epsilon.
\end{aligned}$$

Remark 1. Combining the upper and lower bounds on $\Phi_{N_m^{b_m}}(\cdot)$ derived in Lemma 2 with the lower and upper bounds of Theorem 3 yields lower and upper bounds on $\mathbb{P}_{\text{out}}^{m,m}(\theta, d_f)$, respectively, which are in terms of the system parameters.

VI. NUMERICAL RESULTS

In this section, we present some simulation results and compare the results with the obtained upper and lower bounds. Throughout this section, the simulation results are generated by $10^5 - 10^6$ realizations. We also compare our results with the bounds derived in [15] for the case in which there is no backhaul constraint. The considered setup is a two-tier network in a circle of radius $R = 1$ Km with the MBS located at the center. In the ensuing plots, unless otherwise stated, the default values in Table I are used.

To evaluate the upper and lower bounds stated in Theorems 1 and 2, we need to compute the values of $\{p_i\}_{i=-t}^{t-t}$ and $\{p'_i\}_{i=-t}^{t-t}$, respectively. The values of $\{p_i\}$ are given in Lemma 1 of [15]. As discussed in Appendix A, for small values of κ , the MUs in $\mathcal{U}_m^{\text{out}}(b_m)$ have a near-uniform distribution.

TABLE I
SIMULATION PARAMETERS

Sym.	Description	Default Values
λ_f	density of FAPs	$5 \times 10^{-6} \text{ m}^{-2}$
μ_f	density of femto users	$5 \times 10^{-3} \text{ m}^{-2}$
μ_m	density of macrocell users	$40 \times 10^{-6} \text{ m}^{-2}$
δ	ring width of FUs placement	5 m
r_f	ring internal radius of FUs placement	10 m
α	path loss exponent	4
T	SIR threshold level	2
n_s	number of subbands	32
n_h	number of subchannels in each subbands	1024
η	power ratio between FAPs and MBS	40
κ	handover parameter	0.08

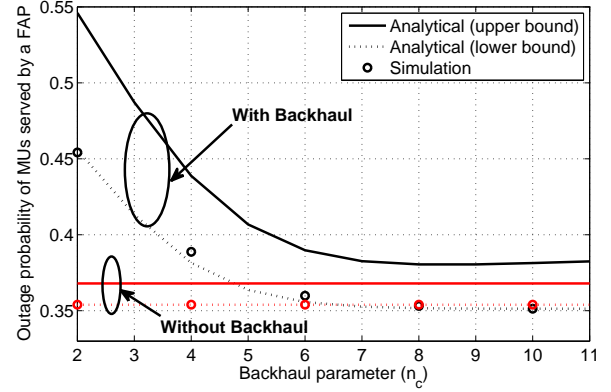


Fig. 3. Outage probability of an MU served by an FAP (at distance of 800 m from the MBS) as a function backhaul parameter n_c .

Therefore, the same Lemma 1 from [15] also provides a reasonable approximation for the values of $\{p'_i\}$.

Fig. 3 shows the effect of the backhaul capacity n_c on the outage probability experienced by the MUs serviced by a FAP located at $d_f = 800$ m from b_m . Increasing the backhaul capacity n_c results in statistically more MUs being serviced by FAPs, which in turn reduces the cross-tier interference experienced by users served by the FAPs. At the same time, this will increase the co-tier interference. However, from the figure, the cross-tier interference is the dominant term compared to the co-tier one. Also, it can be observed that as n_c increases, the backhaul-constraint bounds converge to those of without restriction, computed in [15]. It should be mentioned that for all values of n_c , the bounds are consistent with the simulation results, which confirm the accuracy of the derived analytical bounds.

Fig. 4 shows the outage probability experienced by the MUs serviced by an FAP located at $d_f = 800$ m from b_m as a function of the backhaul parameter n_c , for different values of μ_f , the FUs' density. Obviously, as μ_f increases, the interference caused by FUs also increases. This will increase the outage probability of the MUs serviced by the FAPs. For large values of n_c , the effect of backhaul constraint fades away, and since the dominant cross-tier interference does not depend on μ_f , the curves converge together.

Fig. 5 shows the average outage probability experienced by MUs as a function of n_c , for two different values of μ_m , the

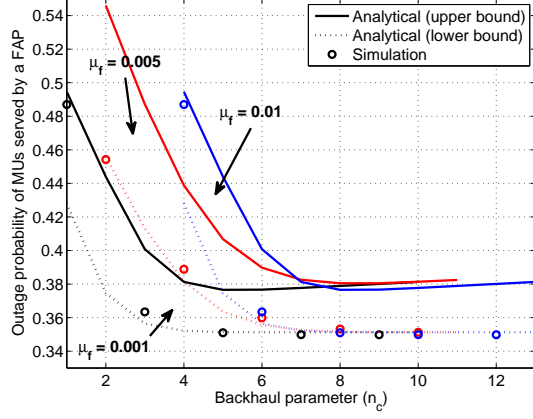


Fig. 4. Outage probability of an MU served by an FAP as a function backhaul parameter n_c for different FUs densities.

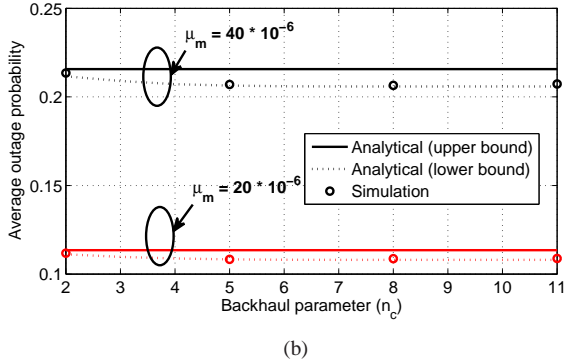
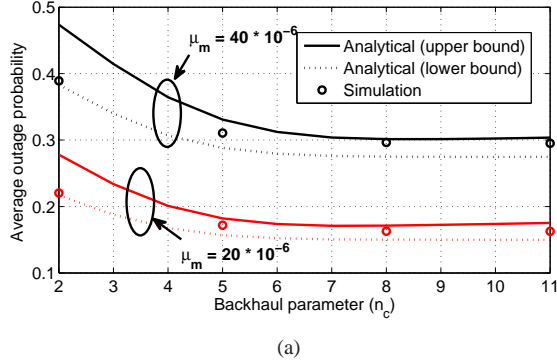


Fig. 5. Outage probability of MUs as a function of the backhaul parameter n_c for different MUs densities a) MUs served by FAPs b) MUs served by the MBS.

MUs' density. Increasing μ increases both cross- and co-tiers interferences, and hence results in higher outage probabilities.¹

Fig. 6 shows the average outage performance of MUs as a function of handover parameter κ and compares the results to the case of no backhaul constraints. For the case in which backhaul constraint is present, it is assumed that $n_c = 3$. As it can be observed, in contrast to the downlink scenario [2], in

¹For plotting the average outage probability experienced by MUs served by the FAPs, we take the expected values of the upper and lower bounds obtained in Theorems 1 and 2 by considering the randomness in d_f .

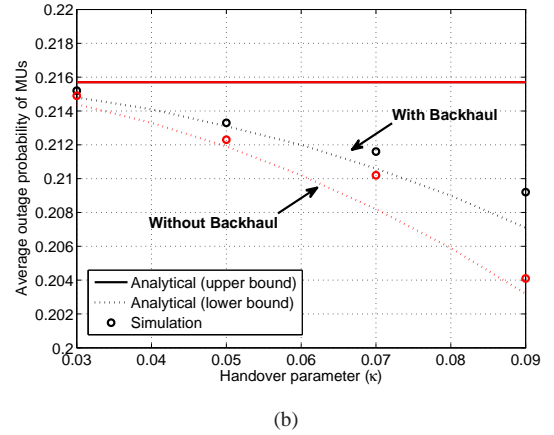
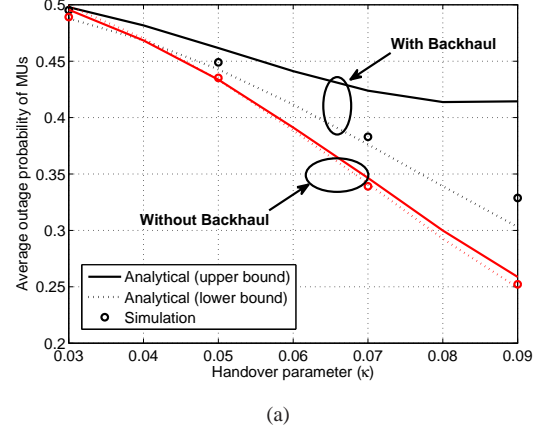


Fig. 6. Outage probability of MUs as a function of the handover parameter κ for the cases of with and without backhaul constraints a) MUs served by FAPs b) MUs served by the MBS.

both cases the outage probability is a monotonic function of κ . As explained in [15], the difference between the uplink and downlink arises from the fact that in the downlink scenario, as the MUs get farther away from the MBS, their received powers decrease and hence SIRs decrease as well. On the other hand, in the uplink communication, as they get farther away from the MBS, due to the power control, their transmit powers increase as well to compensate for the path loss. Naturally, increasing the handover parameter increases the number of MUs covered by FAPs and hence lowers the co-tier interference. Note that while the gap between the upper and lower bounds widens as κ increases, the lower bound follows the simulation results for all values of κ .

Fig. 7 shows the outage probability of MUs served by FAPs as a function of the FAP's normalized distance from the MBS, and compares the results with the case of no backhaul restriction. Here $n_c = 3$. As expected, the outage probability in the presence of backhaul is higher than the ideal case where the FAPs have infinite backhaul capacity. The reason is that because of the backhaul constraints fewer MUs are served by the FAPs and this leads to higher cross-tier interference. However, in both cases, at first, the outage probability increases as the MU gets farther from the MBS.

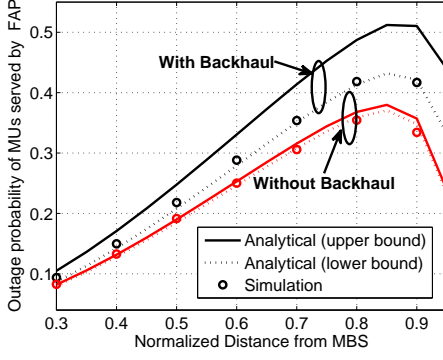


Fig. 7. Outage probability of an MU served by an FAP as a function of the normalized distance of the FAP from the MBS for the cases of with and without backhaul constraints.

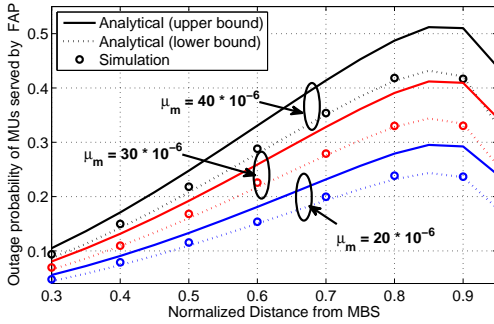


Fig. 8. Outage probability of a MU served by a FAP as a function of the normalized distance of the FAP from the MBS for different MUs densities.

Due to the constant received power assumption at the MBS, as the MU gets farther from the MBS, it will transmit at a higher power, which leads to the degradation in the performance of FUs and also MUs served by the nearby FAPs. However, as the femtocells get close to the fringes of the cell, the outage probabilities start to improve as well. The reason is that femtocells that are far away from the MBS have larger coverage areas and therefore, in those regions most MUs are serviced by nearby FAPs.

Fig. 8 shows the outage probability of MUs served by FAPs as function of the distance between the FAP and the MBS, for different values of MUs' density (μ_m). Obviously, for a fixed backhaul parameter, which is set to 3 in these curves, more MUs being served by the MBS results in higher cross-tier interference and hence higher outage probabilities for MUs served by the FAPs.

VII. CONCLUSIONS

In this paper, we have studied two-tier cellular networks, in which each FAP has a finite backhaul capacity limiting the number of users it can serve. The MUs, FUs and FAPs have all been assumed to have stochastic deployments according to PPPs. We have considered fixed backhaul constraints for FAPs, which limit the number of users each FAP can service. Under these assumptions, we have derived analytical upper and lower bounds on the outage probabilities of MUs serviced by

FAPs and MUs serviced by the MBS. All bounds have been confirmed by our simulation results.

While in our analysis we have assumed that there is only a single MBS, the results can also be applied to real networks with multiple MBSs. To do this extension, we only need to assume that each MU is assigned to its closest MBS and the macro cells employ one of the well-known frequency reuse methods that orthogonalize neighboring cells.

APPENDIX A PARTITIONING \mathcal{S}_m

In this section, we briefly review the partitioning of the coverage area presented in [15]. Consider the MBS b_m and FAP a_f located at distance d from each other. (Refer to Fig. 9.) \mathcal{S}_m denotes the circle of radius R around b_m . The set of points u such that $d(u, a_f)/d(u, b_m) = \kappa'$ or $d(u, a_f)/d(u, b_m) = 1/\kappa'$, where $\kappa' \in (0, 1)$ are two circles of radius $\frac{\kappa' d}{1 - \kappa'^2}$. In Fig. 9, the colored pairs of circles correspond to three different values of κ' .

Consider $\kappa_0, \dots, \kappa_t$ such that $\kappa_0 = \kappa < \kappa_1 < \kappa_2 < \dots < \kappa_t = 1$, and the $2t$ pairs of circles corresponding to $\kappa_0, \dots, \kappa_{t-1}$. These circles do not intersect and in addition to the line corresponding to $\kappa_t = 1$, which corresponds to the set of points u satisfying $d(u, a_f) = d(u, b_m)$, partition \mathcal{S}_m into $2(t+1)$ regions.

APPENDIX B DISTRIBUTION OF USERS IN $\mathcal{U}_m^{\text{ns}}(b_m)$

As a reminder $\mathcal{U}_m^{\text{out}}(b_m)$ denotes the set of users that are covered by the MBS b_m because they do not fall into the coverage area of any of the FAPs. In this appendix, we prove that for κ small the distance of the users in $\mathcal{U}_m^{\text{out}}(b_m)$ to the MBS has an almost uniform distribution. In this section, we assume that $\kappa \leq 0.5$.

Given FAP $a_f \in \mathcal{A}_f$, let $\mathcal{C}(a_f)$ denote the coverage area of a_f . As explained earlier, for FAP a_f at distance d from b_m , $\mathcal{C}(a_f)$ is circle of radius $\frac{\kappa d}{(1 - \kappa^2)}$, whose center is located at distance $\frac{d}{1 - \kappa^2}$ from b_m on the line connecting b_m to a_f .

Consider user u that is located uniformly at random on \mathcal{S}_m . Define \mathcal{E} as the event that u does not fall in the coverage area

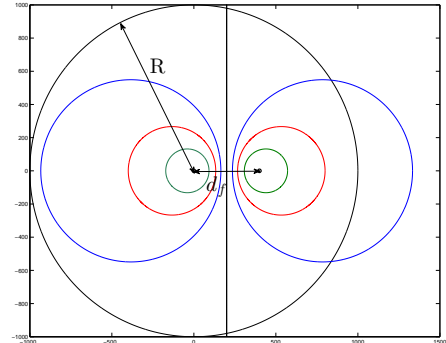


Fig. 9. Partitioning the coverage area

of any of the FAPs, i.e.,

$$\mathcal{E} \triangleq \{u \notin \mathcal{C}(a_f), \forall a_f \in \mathcal{A}_f\}.$$

Let

$$D_u \triangleq d(u, b_m).$$

In this section, we derive the conditional pdf of D_u conditioned on \mathcal{E} , $f_{D_u}(\cdot|\mathcal{E})$. By the Bayes formula,

$$f_{D_u}(d|\mathcal{E}) = \frac{f_{D_u}(d) P(\mathcal{E}|D_u = d)}{P(\mathcal{E})}. \quad (\text{B.1})$$

Since u is drawn uniformly at random, $f_{D_u}(d) = \frac{2d}{R^2}$. On the other hand, since the FAPs are drawn according to a PPP of density λ_f , we have

$$\begin{aligned} P(\mathcal{E}|D_u = d) &= \sum_{n=0}^{\infty} P(\mathcal{E}, N_{\text{fap}} = n | D_u = d) \\ &= \sum_{n=0}^{\infty} p_{N_{\text{fap}}}(n) (P(u \notin \mathcal{C}(a_f) | D_u = d))^n \\ &= \sum_{n=0}^{\infty} e^{-\bar{n}_{\text{fap}}} \frac{(\bar{n}_{\text{fap}})^n}{n!} (P(u \notin \mathcal{C}(a_f) | D_u = d))^n \\ &= e^{-\bar{n}_{\text{fap}} (1 - P(u \in \mathcal{C}(a_f) | D_u = d))} \\ &= e^{-\bar{n}_{\text{fap}} P(u \in \mathcal{C}(a_f) | D_u = d)}. \end{aligned} \quad (\text{B.2})$$

To compute $P(u \in \mathcal{C}(a_f) | D_u = d)$ consider user u at distance d from b_m and FAP located at distance r from b_m . (Refer to Fig. 10.) In order for u to be covered by a_f , d should satisfy

$$\frac{r}{1-\kappa^2} - \frac{r\kappa}{1-\kappa^2} \leq d \leq \frac{r}{1-\kappa^2} + \frac{r\kappa}{1-\kappa^2},$$

or

$$(1-\kappa)d \leq r \leq (1+\kappa)d.$$

Given $r \in ((1-\kappa)d, (1+\kappa)d)$, the angle between the lines (b_m, a_f) and (b_m, u) should be within $(-\theta, \theta)$, where

$$\cos(\theta) = \frac{d^2 + (\frac{r}{1-\kappa^2})^2 - (\frac{\kappa r}{1-\kappa^2})^2}{\frac{2dr}{1-\kappa^2}} = \frac{d^2(1-\kappa^2) + r^2}{2dr}. \quad (\text{B.3})$$

Let $r = d(1+\rho)$, where $\rho \in (-\kappa, \kappa)$. Employing this change of variable, it follows from (B.3) that

$$\cos(\theta) = 1 - \frac{\kappa^2 - \rho^2}{2(1+\rho)},$$

and

$$\begin{aligned} \sin^2(\theta) &= \frac{\kappa^2 - \rho^2}{2(1+\rho)} \left(2 - \frac{\kappa^2 - \rho^2}{2(1+\rho)}\right) \\ &= \kappa^2 - \rho^2 \left(1 - \frac{\rho}{2(1+\rho)} - \frac{\kappa^2 - \rho^2}{4(1+\rho)^2}\right). \end{aligned}$$

Therefore, since for $0 \leq x \leq 1$, $1-x \leq \sqrt{1-x} \leq 1$, we have

$$\sqrt{\kappa^2 - \rho^2} \left(1 - \frac{\rho}{2(1+\rho)} - \frac{\kappa^2 - \rho^2}{4(1+\rho)^2}\right) \leq \sin(\theta) \leq \sqrt{\kappa^2 - \rho^2}. \quad (\text{B.4})$$

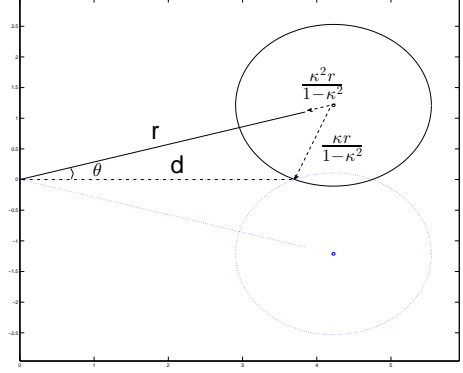


Fig. 10. User u located at distance d from b_m falling in the coverage area of a_f at distance r from b_m .

But,

$$\frac{\rho}{2(1+\rho)} + \frac{\kappa^2 - \rho^2}{4(1+\rho)^2} \leq \frac{\kappa}{2(1-\kappa)} + \frac{\kappa^2}{4(1-\kappa)^2} \leq 2\kappa, \quad (\text{B.5})$$

where the last line follows from our assumption that $\kappa \leq 0.5$. And,

$$\int_{-\kappa}^{\kappa} 2(1+\rho) \sqrt{\kappa^2 - \rho^2} d\rho = \pi \kappa^2. \quad (\text{B.6})$$

Therefore, since $P(u \in \mathcal{C}(a_f) | D_u = d) = \frac{d^2}{\pi R^2} \int_{-\kappa}^{\kappa} 2(1+\rho) \sin(\theta) d\rho$, combining (B.4), (B.5) and (B.6), it follows that

$$(1-2\kappa) \frac{d^2 \kappa^2}{R^2} \leq P(u \in \mathcal{C}(a_f) | D_u = d) \leq \frac{d^2 \kappa^2}{R^2}. \quad (\text{B.7})$$

Combining (B.2) and (B.7) yields

$$e^{-\bar{n}_{\text{fap}} d^2 \kappa^2 / R^2} \leq P(\mathcal{E} | D_u = r) \leq e^{-\bar{n}_{\text{fap}} d^2 \kappa^2 (1-2\kappa) / R^2}, \quad (\text{B.8})$$

and $P(\mathcal{E}) = \int_0^R \frac{2r}{R^2} P(\mathcal{E} | D_u = d) dr$ satisfies

$$\frac{1 - e^{-\kappa^2 \bar{n}_{\text{fap}}}}{\kappa^2 \bar{n}_{\text{fap}}} \leq P(\mathcal{E}) \leq \frac{1 - e^{-(1-2\kappa) \kappa^2 \bar{n}_{\text{fap}}}}{(1-2\kappa) \kappa^2 \bar{n}_{\text{fap}}}. \quad (\text{B.9})$$

Finally, from (B.1), (B.8) and (B.9),

$$f_{D_u}(d|\mathcal{E}) \geq \frac{(1-2\kappa) \kappa^2 \bar{n}_{\text{fap}} e^{-\bar{n}_{\text{fap}} d^2 \kappa^2 / R^2}}{1 - e^{-(1-2\kappa) \kappa^2 \bar{n}_{\text{fap}}}} \left(\frac{2d}{R^2}\right), \quad (\text{B.10})$$

$$f_{D_u}(d|\mathcal{E}) \leq \frac{\kappa^2 \bar{n}_{\text{fap}} e^{-\bar{n}_{\text{fap}} d^2 (1-2\kappa) \kappa^2 / R^2}}{1 - e^{-\kappa^2 \bar{n}_{\text{fap}}}} \left(\frac{2d}{R^2}\right). \quad (\text{B.11})$$

Note that for $\kappa \ll 1$, the lower bound and the bound bound in (B.10) and (B.11), respectively, converge to $2d/R^2$, which corresponds to the uniform distribution over a circle of radius R .

REFERENCES

- [1] M. Haenggi, J. G. Andrews, F. Baccelli, O. Dousse, and M. Franceschetti. Stochastic geometry and random graphs for the analysis and design of wireless networks. *IEEE Journal on Sel. Areas in Commun.*, 27(7):1029–1046, 2009.

- [2] W. C. Cheung, T. Q. S. Quek, and M. Kountouris. Throughput optimization, spectrum allocation, and access control in two-tier femtocell networks. *IEEE Journal on Sel. Areas in Commun.*, 30(3):561–574, 2012.
- [3] H. S. Jo, Y. J. Sang, P. Xia, and J. G. Andrews. Heterogeneous cellular networks with flexible cell association: A comprehensive downlink SINR analysis. *IEEE Trans. on Wireless Commun.*, 11(10):3484–3495, 2012.
- [4] F. Baccelli and S. Zuyev. Stochastic geometry models of mobile communication networks. *Frontiers in Queueing*, pages 227–243, 1997.
- [5] F. Baccelli, M. Klein, M. Lebourges, and S. Zuyev. Stochastic geometry and architecture of communication networks. *Telecommun. Sys.*, 7(1-3):209–227, 1997.
- [6] T. X. Brown. Cellular performance bounds via shotgun cellular systems. *IEEE Journal on Sel. Areas in Commun.*, 18(11):2443–2455, 2000.
- [7] H. S. Dhillon, R. K. Ganti, F. Baccelli, and J. G. Andrews. Modeling and analysis of k-tier downlink heterogeneous cellular networks. *IEEE Journal on Sel. Areas in Commun.*, 30(3):550–560, 2012.
- [8] S. Mukherjee. Distribution of downlink sinr in heterogeneous cellular networks. *IEEE Journal on Sel. Areas in Commun.*, 30(3):575–585, 2012.
- [9] W. C. Cheung, T. Q. S. Quek, and M. Kountouris. Throughput optimization, spectrum allocation, and access control in two-tier femtocell networks. *IEEE Journal on Sel. Areas in Commun.*, 30(3):561–574, 2012.
- [10] B. Yu, S. Mukherjee, H. Ishii, and L. Yang. Dynamic TDD support in the LTE-B enhanced local area architecture. In *Proc. Globecom Workshop on Heterogeneous and Small Cell Networks*, pages 585–591, Dec. 2012.
- [11] V. Chandrasekhar and J. G. Andrews. Uplink capacity and interference avoidance for two-tier femtocell networks. *IEEE Trans. on Wireless Commun.*, 8(7):3498–3509, 2009.
- [12] N. Chakchouk and B. Hamdaoui. Uplink performance characterization and analysis of two-tier femtocell networks. *IEEE Trans. on Veh. Tech.*, 61(9):4057–4068, 2012.
- [13] W. Bao and B. Liang. Uplink interference analysis for two-tier cellular networks with diverse users under random spatial patterns. In *Proc. of IEEE/CIC Int. Conf. on Commun. in China (ICCC), Xian, China*, 2013.
- [14] W. Bao and B. Liang. Understanding the benefits of open access in femtocell networks: Stochastic geometric analysis in the uplink. In *Proc. of the 16th ACM Int. Conf. on Mod., Ana. & Sim. of Wireless and Mobile Sys.*, pages 237–246, 2013.
- [15] Z. Zeinalpour-Yazdi and S. Jalali. Outage analysis of uplink two-tier networks. Accepted for publication in *IEEE Trans. on Commun.*, 2014.
- [16] H. ElSawy and E. Hossain. On stochastic geometry modeling of cellular uplink transmission with truncated channel inversion power control. *IEEE Trans. on Wireless Commun.*, 13(8):4454–4469, Aug. 2014.
- [17] P. Xia, V. Chandrasekhar, and J. G. Andrews. Open vs. closed access femtocells in the uplink. *IEEE Trans. on Wireless Commun.*, 9(12):3798–3809, 2010.
- [18] T. Elkourdi and O. Simeone. Femtocell as a relay: An outage analysis. *IEEE Trans. on Wireless Commun.*, 10(12):4204–4213, Dec. 2011.
- [19] D. W. K. Ng, E. S. Lo, and R. Schober. Energy-efficient resource allocation in multi-cell OFDMA systems with limited backhaul capacity. *IEEE Trans. on Wireless Commun.*, 11(10):3618–3631, Oct. 2012.
- [20] I. V. Loumriotis, E. F. Adamopoulou, K. P. Demestichas, T. A. Stamatiadis, and M. E. Theologou. Dynamic backhaul resource allocation: An evolutionary game theoretic approach. *IEEE Trans. on Commun.*, 62(2):691–698, Feb. 2014.
- [21] E. Lance and G. K. Kaleh. A diversity scheme for a phase-coherent frequency-hopping spread-spectrum system. *IEEE Trans. on Commun.*, 45(9):1123–1129, 1997.